REAR FUSELAGE FLOW CHARACTERISTICS FOR A COMPLETE WING-BODY CONFIGURATION AT TRANSONIC CONDITIONS

by

E. Coustols, A. Séraudie & A. Mignosi

CERT-ONERA, Aerothermodynamics Department, Toulouse, France.

Abstract

That study deals with experiments conducted in the transonic, pressurized T2 wind tunnel of CERT. The 1/80th scale model of a modern subsonic transport aircraft was handled in the test section using a finsting. It consisted of a fuselage, a detachable horizontal rear stabilizer, a belly fairing and tip-truncated wings; those latter were computed by Aerospatiale in order to reproduce the correct downwash in the rear fuselage region. Tests were carried out at a free stream Mach number of 0.82 and a Reynolds number based upon the model chord length of close to 2.5 million.

Various measurements were performed, mainly in the vicinity of the fuselage downstream rear part: oil-flow visualisations; pressure distributions; boundary layer surveys along the fuselage symmetry lines and some lateral lines using a Laser Doppler Anemometry system; and near wake surveys with both pressure and velocity measurements.

Those experiments were aimed at scrutinizing the flows developing along the rear part of a fuselage, in a configuration very close to flight applications.

Introduction

Experimental as well as numerical work on rear parts of fuselage have been developed at CERT/ONERA for these last years. That work has several goals:

- first of all, to reach a better understanding of the external and wall flows developing along the fuselage of a commercial-type subsonic aircraft for different model configurations: "Fuselage without stabilizer", "Fuselage with stabilizer" and "complete wing-body";
- secondly, to generate an important data base (pressure distributions, boundary layer and near-wake surveys with either velocity or pressure measurements or both) necessary for validating inviscid and viscous codes used and developed at ONERA;
- and lastly, to forecast possible three-dimensional separation (storage of fluid which leads to important viscous drag increase) and, if necessary, definition of passive devices as a means to "control" the flow in those areas.

Consequently, after carrying out detailed experimental work on both "Fuselage without and with horizontal stabilizer",[1,2] a second set of experiments has been launched in order to go closer to flight applications: indeed, a whole wing-body configuration of a modern transonic transport aircraft has been considered. The aim of this specific experimental approach has been to explore the role played by the horizontal stabilizer and the wing lift on rear-fuselage flows, and to look at the interaction between the wake coming from the tip-truncated wings and the boundary layer developing along the fuselage.

The experiments reported here were conducted in the test section of the CERT T2 wind tunnel, which is transonic, pressurized, and has self adaptive walls. Tests were performed at a stagnation pressure close to 2.1 bar, at ambient temperature and at a free stream Mach number of 0.82. The Reynolds number, based on the aerodynamical chord length of the model, was close to 2.5 million. Although that Reynolds number is one order of magnitude less than that corresponding to flight or cruise conditions, its value is in perfect agreement with those recorded among the numerous industrial wind tunnel applications. Furthermore, computations showed that the fuselage viscous flow pattern was quite similar whatever value of the Reynolds number, based upon either test or flight conditions.

Several measurements have been performed in order to detail the rear fuselage flow characteristics: oil-flow visualisations; pressure distributions; boundary layer surveys along the upper and lower symmetry lines using the three-dimensional Laser Doppler Anemometry (LDA) system; and wake surveys with both pressure and velocity measurements in two planes located at approximately one and two diameters downstream of the fuselage base.

Wind tunnel conditions

Experimental Set-Up - Model

The T2 wind tunnel at CERT/DERAT

The T2 wind tunnel is a closed-circuit, induction-driven facility capable of runs between 30 and 120 seconds. It is pressurized, transonic, and cryogenic, and it has self-adaptive walls. Dry air is injected at ambient temperature and cooled by an injection of liquid nitrogen for cryogenic conditions.[3] The standard operating range is: M_∞: 0.6-0.9, Pi_∞: 1.3-3.0 bar and Ti_∞: 120-300 K.

The test section of the wind tunnel measures 0.39 m wide, 0.37 m high and 1.42 m long. The flexible top and bottom walls avoid transonic blockage and minimize wall interference effects. These walls can be controlled using either a two- or three-dimensional strategy;[4,5] they are moved by 16 hydraulic jacks acting upon invar steel sheets, allowing displacement in 0.2 mm increments up to a maximum variation of 25 mm. The tunnel's adaptive wall capability allows relatively large models to be studied and provides very accurate results.

Besides its ability to provide high Reynolds number values, this wind tunnel is also particularly suitable for studying rear fuselage flow because its three-dimensional LDA system[6,7] allows the recording of detailed secondary fields that are crucial for measuring vortex flows.

Model

The 1/80th-scale model of a modern transonic transport aircraft was designed and manufactured at ONERA/IMF Lille. It consisted of a fuselage, a detachable horizontal rear stabilizer, a belly fairing and tip-truncated wings. The cylindrical fuselage was 0.733 m long and 0.070 m in diameter. The model differed from the full-scale aircraft in having no horizontal stabilizer shield and no gap between the horizontal stabilizer and the fuselage; moreover, the shape of the belly fairing was not exactly the full-scale aircraft one and there was no wing/fuselage onglet. Later experiments showed that these small modifications do not affect the main characteristics of the rear-fuselage flow, although the absence of gap would impede a possible connection between the lower and upper parts of the fuselage.

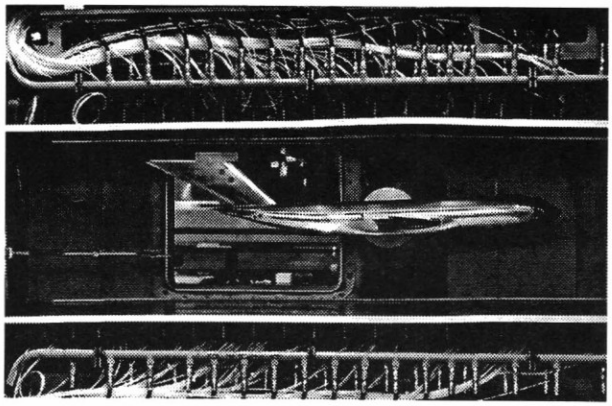

Figure 1: *View of the model in the T2's test section.*

Because of the size of the wind tunnel cross section, the real wing sized at the right scale, could not be considered. So, tip-truncated wings with with exactly the same chord length at the wings/fuselage junction, were computed by Aerospatiale.[8] For correct qualification of the aerodynamic field on the fuselage rear section, those wings had to be defined so that the pressure field on the fuselage and the position of the wake of the wing on the fuselage looked like those obtained with the real wing, for the wind tunnel conditions; furthermore, the transverse evolution of the lift coefficient was reproduced. So, the correct downwash on the fuselage should be correctly represented.

Experimental set-up

The model was handled in the test section using the same fin-sting as the one used for the "Fuselage with or without stabilizer" configurations[1,2] (figure 1). The model fin was geometrically different from the full-scale aircraft fin, but both the chord at the fuselage/fin junction and the sweep angle of the leading edge were correct.

The sting induced interferences along the centreline of the wind tunnel, in the area where the upswept rear-fuselage would be located, but the tunnel's flexible upper and lower walls allowed this interference to be cancelled out on the fuselage axis. Velocity measurements performed during this stage of the experiment verified that the residual disturbances were small.[5] Details regarding wall adaptation are given later.

Instrumentation

The model's fuselage (cylindrical part as well as belly fairing) was fitted with 142 static pressure taps, 115 of which were located on the left hand-side of the rear part, along the last 32% of its fuselage length. For two streamwise sections, taps located in the same horizontal plane helped verify that the model was not set askew. By recording so many pressure measurements in this downstream part of the fuselage it was possible to define, fairly exactly, both the streamwise evolution of pressure along the symmetry lines and the azimuthal distribution of the pressure–definitions that proved critical when examining the influence of the horizontal stabilizer on the external flow.

Furthermore, the lower and upper sides of the left hand side tip-truncated wing had 44 pressure taps, distributed in three sections, located at 65 mm, 105 mm and 145 mm from the fuselage axis; the corresponding local chords are 117 mm, 96.6 mm and 84.5 mm respectively.

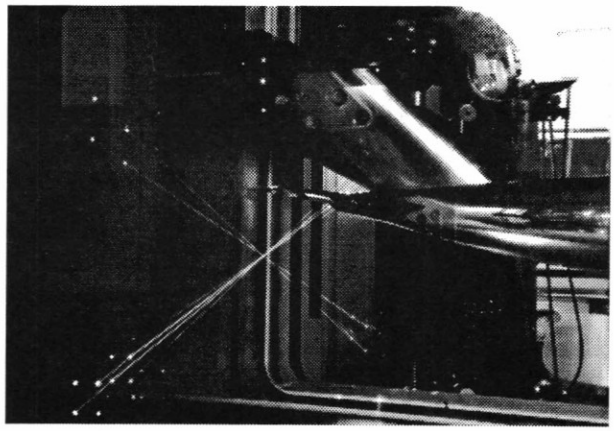

Figure 2: *Glance at the instrumentation.*

For wake surveys, a specific pressure rake has been constructed: it was 84 mm wide and had two decks, the upper one consisting of 15 total pressure probes and the lower one of 6 static ones; all the probes were

set at equal distance one from each other (figures 1& 2). This rake was calibrated, without the model, at the beginning of the experiments but, because of its obstruction, some residual corrections were applied to the static values. That pressure rake allows to cover the whole wake plane survey within a single run.

The three-dimensional LDA system was used for boundary layer and wake surveys (figure 2). The diameter of the measuring volume, tightly related to the intersection of the three coloured beams as well as their waists, was close to 130 μm for any configuration (forward- or backward-scattering). Regarding nearer wall approaches, using the forward-scattering mode (tangential approach, for the symmetry lines of the model), one could go as close as 0.3-0.4 mm to the wall; however, in the backward-scattering mode (normal approach, mid-lateral line on the fuselage), the shortest distance to the wall was 3.0 mm.

Test conditions

Tests were carried out at a stagnation pressure of 2.1 bar, at ambient temperature (300 K), for a free stream Mach number of 0.82. That led to a Reynolds number R_c based upon the aerodynamical chord length of the model (0.091 m) of close to 2.5 million.

Transition was tripped on the fuselage (carborundum band, average height: 45 μm at 12 mm from the nose), on the lower and upper sides of the horizontal stabilizer (carborundum band, average height: 35 μm at 5% of the local chord length) and on the lower and upper sides of the wings (carborundum band, average height: 45 μm at 5% of the local chord length), but natural transition occurred on the vertical fin.

For all this set of experiments, the fuselage axis was set at α=2.5°, whilst the horizontal stabilizer was set at α_e=-2° with respect to the Reference Horizontal Fuselage line. That configuration is representative of the average cruise conditions.

Wall adaptation process and Measurements

In order to reproduce the external flow around the model as accurately as possible, the adaptation of the flexible walls of the test section had to be calculated according to methods developed at DERAT.[4,5] The upper and lower flexible walls had to be adapted to the presence of the model and of the four walls boundary layers, knowing that the side ones are parallel; final adjustments, using the linearity assumption, were made to counteract the disturbance caused by the sting.

Because of the location of the tip-truncated wings and of the induced downwash, it was necessary to re-set in a new position the top and bottom walls of the test section in comparison to the "Fuselage with stabilizer" configuration. Indeed, in order to counteract the wing lift, the displacement of the flexible walls has to be greater. Great care has been taken in order to ensure the correct pressure distribution on the model as well as the quality of the results.

When the adjustments had been made, the following measurements were done:
- oil-flow visualisations on the rear part of the fuselage, on the tip-truncated wings and on the horizontal and vertical stabilizers.
- streamwise pressure distributions on the rear part of the fuselage, along the upper and lower symmetry lines and on the tip-truncated wings; azimuthal evolution of the pressure for given streamwise sections.
- boundary layer surveys at several streamwise abscissae along the symmetry lines of the model using the forward-scattering LDA mode, and for several azimuthal positions using the backward-scattering Laser Doppler Anemometry mode.
- wake surveys through both velocity and pressure measurements, in two planes located at approximately one and two diameters downstream of the fuselage base. Regarding velocity measurements, a complete plane (~ 1100-1200 points) was investigated at 60 mm downstream of the fuselage base, while half of the measurement points (500-600) was performed in one half of the wake at the plane located at 120 mm downstream of the base.

Results and discussions

Pressure field

The streamwise evolution of the pressure coefficient is plotted in figure 3 at three sections: Y=65 mm, 105 mm and 145 mm from the fuselage axis.

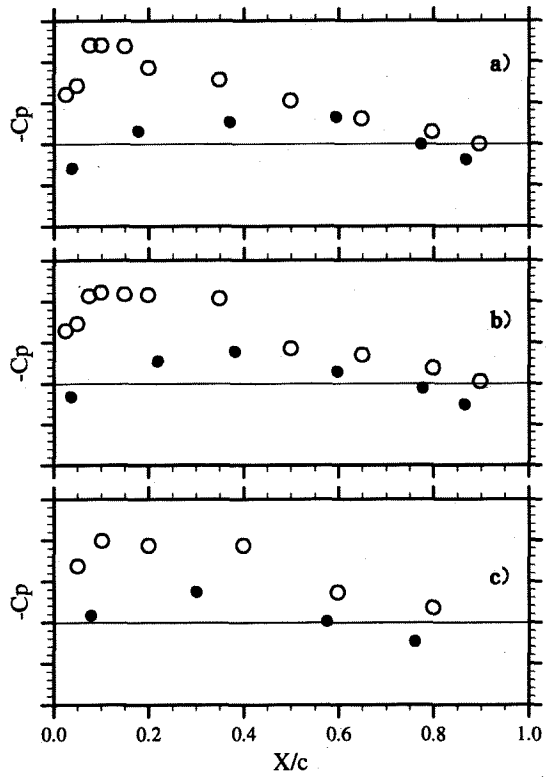

Figure 3: *Pressure distribution on the tip-truncated wing: a) Y=65 mm; b) Y=105 mm c) Y=145 mm; o: Upper side •: Lower side (— Cp=0).*

These distributions were in agreement with those

recorded by industrial companies on comparable wing-body models†. That implies, first of all that the adaptation process has been carried out correctly, and secondly that the tip-truncated wings have been well designed.

Measurements showed the existence of a shock wave on the upper part of the tip-truncated wings and its transverse evolution, leading to a splitting within the internal wing (figure 4). Local Mach numbers up to 1.5 were recorded. The number of pressure taps was not sufficient to capture correclty the location of the shock wave; oil-flow visualisations allowed to complete that description, yet.

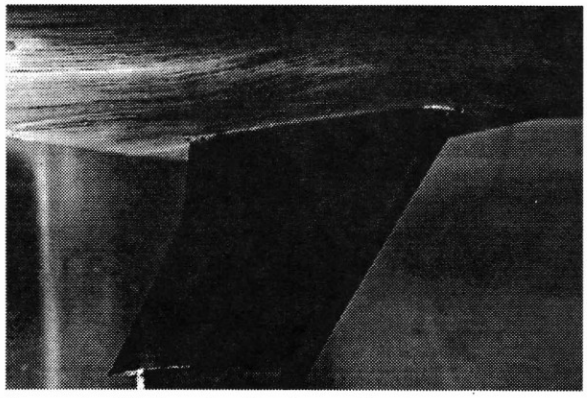

Figure 4: *Oil-flow visualisation on the tip-truncated wing.*

Once the shock wave footprint estimated, the lift coefficient has been computed at the three Y-spanwise locations; compared to the theoretical evolution versus the span, the correct tendancy has been obtained.

The concentrations of pressure taps on the rear part of the fuselage created a good picture of the pressure field in that region. Plots of the contours of constant pressure coefficient are given in figure 5. Comparisons have been made with the configuration without wings and belly fairing, but at two different values of the angle of attack of the model, i.e α=2.5° and 0°.

Whatever configuration, the flow decelerated just ahead of the leading edge of the fin/fuselage junction. Downstream of that area, the flow then accelerated as far as the maximum cross-section of the horizontal stabilizer footprint. Comparisons with the "Fuselage with horizontal stabilizer" configuration when the model was set at α=2.5° showed some discrepancies, especially along the lower part of the fuselage. In fact, the wings induced such a downwash that the apparent angle of attack of the horizontal stabilizer is smaller. However, when comparing to the configuration with the model set at α=0° (case c) of figure 5) the agreement between the two experimental pressure distributions was very satisfactory.

The wing lift influence was clearly visible on the pressure distribution over the fuselage (figure 6); the truncated wings induced a very strong acceleration of the flow, especially in their neighbourhood.

†Aerospatiale - Private communication

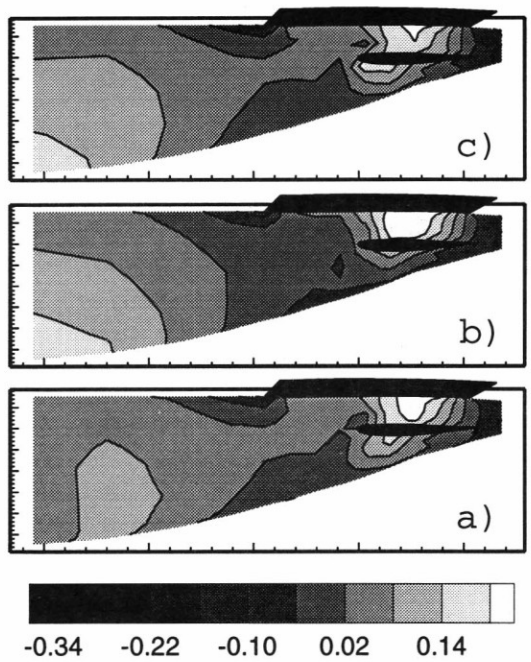

Figure 5: *Colored contours of constant pressure coefficient (-Cp) on the rear fuselage a)Wing-body configuration: α=2.5° α_e=-2° b) Fuselage alone with horizontal stabilizer: α=2.5° α_e=-2° c) Fuselage alone with horizontal stabilizer: α=0° α_e=-2°.*

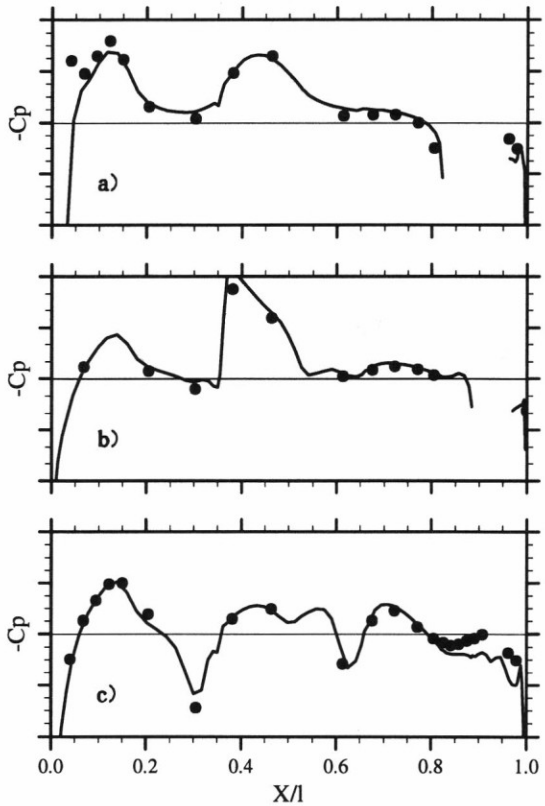

Figure 6: *Pressure distribution along the fuselage: a) Upper symmetry line; b) Mid-lateral line (above the wing/fuselage junction) c) Lower symmetry line (— Cp=0); •: Experiments — Inviscid flow computations.*

The rear part of the belly fairing slowed down the flow at the beginning of the fuselage upsweep, and thus reduced the adverse pressure gradient on the upswept lower part of the fuselage.

Comparisons were performed with inviscid flow computations performed at ONERA. The potential flow was calculated by using a panel method, developed at Aerospatiale;[9] it is a source-vortex method using both skin and skeleton panels bearing either sources or vortices of constant strength.[2,9]

Computed pressure evolutions are thus given in figure 6; the blanks on the full dark lines refer to either the vertical or horizontal stabilizer footprints. A very good agreement existed on most of the fuselage and of its rear part; that feature confirms that the adaptation procedure has been perfectly undertaken.

Some discrepancies were well evidenced along the lower symmetry line both on the pressure level and on the intensity of the pressure gradient. This is due to, first of all, the absence of coupling between inviscid and viscous calculations and, secondly, to a rather thick boundary layer in this area due to the upswept fuselage.

Moreover, the streamwise pressure gradient along the lower symmetry line is almost equal to zero, downstream of X/l=0.8. That would suggest that the rapid growth of the boundary layer in that area balanced the decrease of the fuselage cross-section. The measured as well as computed pressure evolutions appear somewhat "chaotic" around X/l=0.93 (figure 6c); this is due to the local geometrical inflexion of the lower symmetry line.

Wall pattern

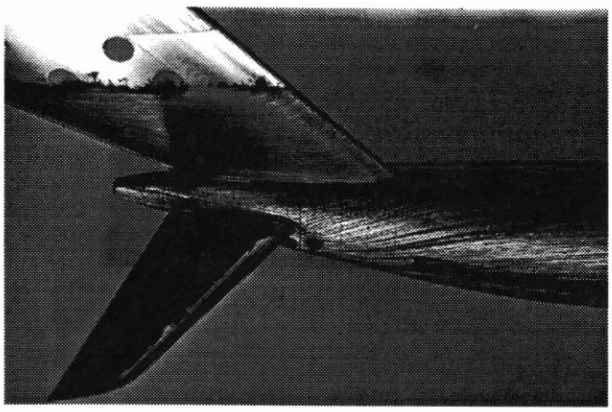

Figure 7: *Oil-flow visualisation - View from above.*

Oil-flow visualisations were performed on different parts of the model. They were very useful in that set of experiments since they allowed to verify the efficiency of transition tripping on the tip-truncated wings as well as on the horizontal tailplane or to find out the splitting of the shock wave on the upper side of the wing; that latter could not be deduced from pressure distribution (see figure 4).

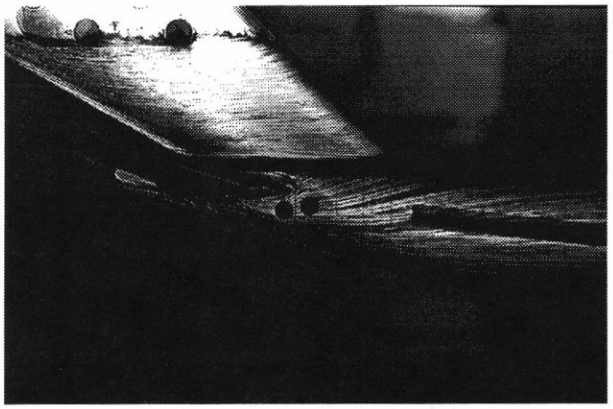

Figure 8: *Oil-flow visualisation - Side view.*

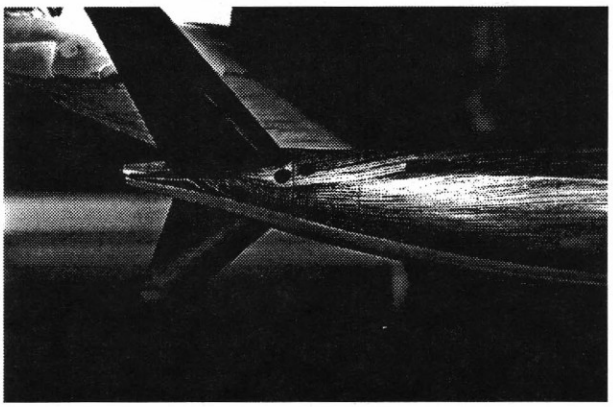

Figure 9: *Oil-flow visualisation - View from below.*

Furthermore, those visualisations allowed to define precisely the wall flow pattern along the fuselage. From some photographs (figures 7, 8 & 9), the following salient features could be observed, such as:
- a rather strong deviation of wall streamlines in the cylindric part of the model, due to the wings;
- a dark triangle area on the lower side of the stabilizer, where oil could gather because of low friction;
- a weak accumulation of wall flow on the upper side of the fuselage, concentrated along the edge of the flat surface, which allows rotation of the horizontal tail;
- a rather strong convergence of wall streamlines inducing an upward motion of wall flow from the lower symmetry line towards the maximum cross-section of the horizontal stabilizer. Such a motion gave rise to a vortex roll-up, the source of which is the upsweep. Its vertical development was restricted because of the tailplane.

Wake surveys

Pressure and velocity measurements were performed in two wake planes, orthogonal to the direction of the free stream velocity X; they are located at 60 mm and 120 mm downstream of the fuselage base, which corresponds to almost one and two diameters, respectively. In these wake surveys, Y=0 refers to as the symmetry plane of the fuselage; the Z-axis ends up the coordinate system.

Therefore, comparisons with the configurations with-

out wings, tested in a preceding campaign,[1,2] will be possible in the furthest plane, for which LDA measurements were only handled.

Pressure rake measurements

The relative variations of the stagnation pressure in the wake, at 120 mm downstream of the fuselage base, are given in figure 10b. Comparisons are made with the configuration without wings (figure 10a).

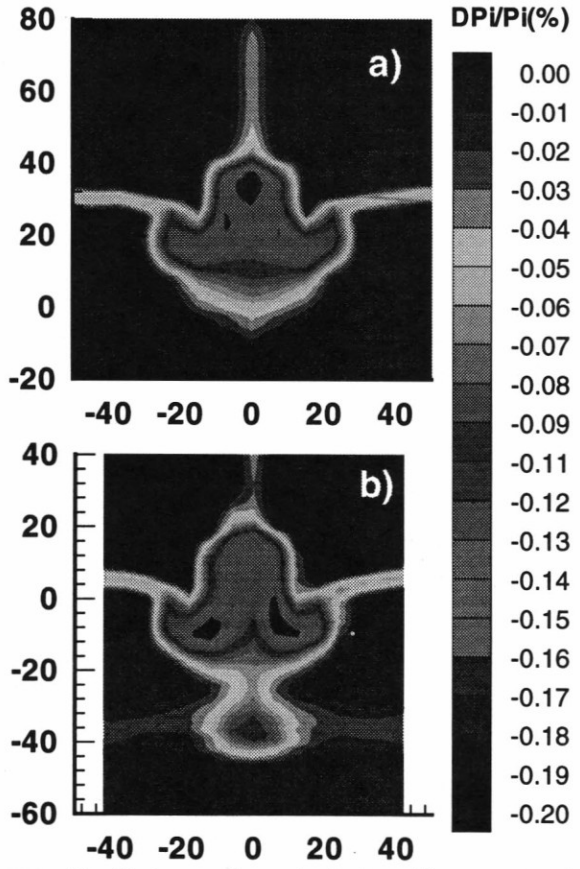

Figure 10: *Contours of constant stagnation pressure loss ($\Delta Pi/Pi$) in the wake a) Fuselage alone with horizontal stabilizer: α=0° α_e=-2° b) Wing-body configuration: α=2.5° α_e=-2°.*

The following comments can be made:

- the symmetry of measurements in the wake plane was rather good and comparable to that recorded for the fuselage alone configuration with or without horizontal stabilizer (see[1,2]);
- the wakes from the vertical and horizontal stabilizers, as well as from the fuselage/wing interaction and the fuselage were clearly evidenced;
- the shape of the wake was different from the configurations without wings; however, its size (height, width) was comparable first of all to the geometry of the fuselage and secondly to that recorded when investigating the "Fuselage/tailplane configuration" with α=0°;
- pressure loss downstream of the tailplane was roughly constant and equal to 6-8%;
- three different defect velocity pockets were recorded in the fuselage wake. The highest one came from both the fuselage base and the convergence of wall flow along the upper edge of the flat surface, which allows rotation of the horizontal tail; the average pressure loss was around 15%. The two lowest ones, symmetrical with regard to the wake axis, seemed to be initiated from the vortex roll-up spreading along the lower part of the fuselage. A maximum deficit of nearly 20% has been recorded.
- in the lower part of the pictures, the wake of the wing itself induced variations of stagnation pressure of about 2-3%, at approximately 4-5 chord length downstream of the wing trailing edge. Nevertheless, a fourth defect velocity pocket, of weaker intensity up to 8-10% could be seen under the fuselage; its existence could be attributed to the wake of the vortex which spred from the wing/fuselage junction. Since the wing/fuselage onglet was not present during the tests, that pressure loss might not be really representative of the real aircraft situation.

The streamwise evolution of the wake between one and two diameters downstream of the fuselage base, did not reveal strong mixing. Of course, the intensity of the pressure loss pockets was slightly weaker at the furthest plane, but the location of the pockets within the wake did not change.

When comparing to the case without wings (figure 10a), the general shape of the fuselage wake has been kept constant which is in agreement with the aforementioned similarity of the isobar contours between the two aerodynamic configurations. In that isobars plot, the sharp peak in the upper part of the fuselage wake could be observed in both configurations. This peak has to be related to strong downwards negative velocities, as it will be discussed later in this paper.

The same defect velocity pockets existed at roughly the same position within the fuselage wake; however, their intensity appeared somewhat weaker for the case without wings. That might be attributed to a stronger vortex roll-up along the lower part of the fuselage due to the presence of the wings and its lift.

3D-LDA measurements - vorticity

The secondary velocity field has been obtained through LDA measurements (forward scattering); surveys in the Z-direction have been performed over 96 mm height. The lateral step of scrutinizing in the Y-direction depends upon the location within the wake plane: 2 mm in the heart of the wake and 3 mm everywhere else.

That secondary velocity field is plotted in figure 11, for the plane located at 60 mm downstream of the fuselage base; it is superimposed to the contours of constant stagnation pressure. It should be noticed that first of all the pressure and the velocity measurements were very consistent, and secondly the flow was perfectly symmetric. The wakes of every part of the model (fin, tailplane, wings, ...) were clearly noticeable in that velocity survey.

Furthermore, the approximate location of the centre of each observed vortex in the fuselage wake has been given with respect to Y- and Z-cordinates.

Downstream of the tip-truncated wings, outside of the main wake of the fuselage, there was a noticeable downward motion of fluid, related to the overall de-

viation of the external flow. A convergence of the wake from the wings towards the symmetry plane of the wake of the model was clear; as a consequence, important vertical velocities were recorded in areas where vortex activity was intense, where Mach numbers were small, i.e. where pressure loss was maximum.

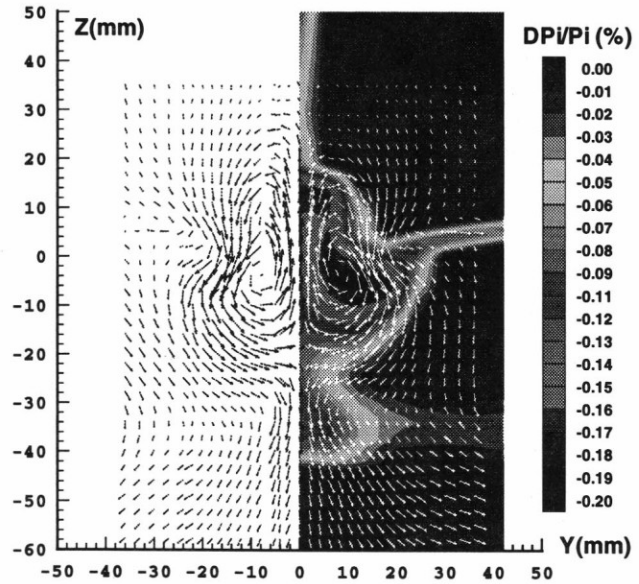

Figure 11: *Secondary velocity field and comparison to the contours of constant stagnation pressure loss ($\Delta Pi/Pi$).*

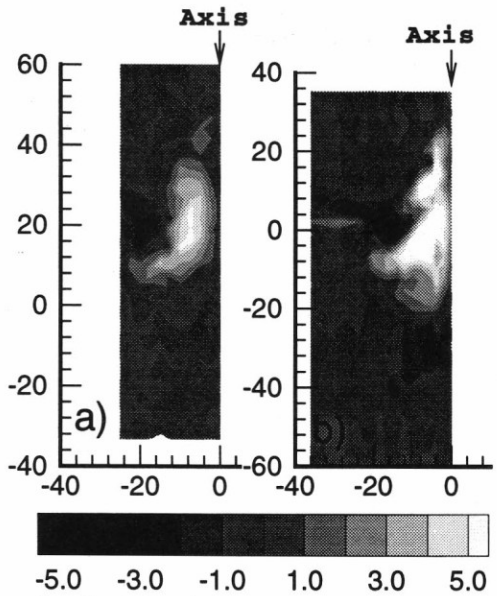

Figure 12: *Contours of constant streamwise component of the rotational (Ω_x) a) Fuselage with horizontal stabilizer: α=0° α_e=-2° b) Wing-body configuration: α=2.5° α_e=-2°.*

Measurements showed the existence of three vortices in each half-wake fuselage plane, compared to two vortices in the configurations without wings.

Two of them were co-rotating, located not very far away from the wake axis. They corresponded to vortex roll-up and convergence of wall flow identified along the fuselage, using oil-flow visualisations; the highest one (Y∼-8 mm, Z∼ 10 mm) has to be related to the interference between the tailplane and rear fuselage flows, whilst the lowest one (Y∼ -10 mm, Z∼ -2 mm) has to be linked to the rear fuselage upsweep.

The third one, contra-rotating (Y∼ -22 mm, Z∼ 2 mm) was located above the tailplane/fuselage junction. Its interaction with the other two vortices created rather large negative velocity components, justifying the sharp shape on the contours of constant stagnation pressure. On the other hand, the junction of the co-rotating vortices induced a prononced upward fluid motion along the wake axis.

At the furthest downstream wake plane, the co-rotating vortices collapsed and produced a unique stronger vortex; the secondary velocity plot was then very similar to that recorded in the configuration without wings (α=0° α_e=-2°) as it can be seen in the contours plot of constant streamwise component of the rotational ($\Omega_x=\partial W/\partial Y-\partial V/\partial Z$).

Such a representation allows to define rather precisely the centre of the different vortex systems downstream of the fuselage (figure 12). Rather weak Ω_x has been recorded at the location of the defect velocity pocket corresponding to the wake of the vortex that develops downstream of the wing/fuselage junction. The overall vorticity seemed to be somewhat stronger than for the configurations without wings.

These wake surveys pointed out the importance and complementarity of pressure and velocity measurements for scrutinizing vortex flows.

Estimations of drag coefficient:

From wake surveys performed through both velocity and pressure measurements, the total drag coefficient of the model could be estimated. Indeed, by considering two planes one upstream of the model (stagnation conditions) and the other one downstream (at 120 mm from the fuselage base), the total drag Cd could be expressed from momentum considerations as:

$$Cd = \frac{1}{\frac{1}{2}S_{ref.}}\int_{wake}\frac{\rho U}{\rho_\infty U_\infty}\left(1-\frac{U}{U_\infty}\right)dS + \frac{1}{\frac{1}{2}\gamma M_\infty^2 S_{ref.}}\int_{wake}\left(1-\frac{P}{P_\infty}\right)dS$$

where the reference surface is the total wing area at the model scale. By considering only first order's terms, the vortex drag component could read:

$$Cd_{vortex} = \frac{1}{\frac{1}{2}S_{ref.}}\int_{wake}\frac{1}{2}\frac{\rho}{\rho_\infty}\frac{(V^2+W^2)}{U_\infty^2}dS$$

In order to estimate the drag coefficient of the fuselage alone, it has been necessary to eliminate the effects of the stabilizers, wings and belly fairing. Some difficulties arose because of the strong interaction of these lifting surfaces with the fuselage. Contributions of the fin as well as the tailplane were taken off, using the same method as the one previously developed for the configurations without wings.[1,2]

However, it has been very difficult to get rid of the contribution of the wing/fuselage junction and belly

fairing, because of the rather strong interaction between them and the fuselage. Then, one ends up with the following data, where ΔCd represents the relative drag variation of the fuselage drag of a given configuration from the total drag of the complete wing-body configuration.

Drag coefficient of the fuselage part only				
$\alpha(^o)$	$\alpha_e(^o)$	Wings	$10^4\ \Delta$ Cd	Cd_{vortex}/Cd
0	-2	No	-0.9	1.1%
2.5	-2	No	-5.0	0.2%
2.5	-2	Yes	—	2.6%

Then, for the configurations without wings, the total drag of the fuselage, mainly pressure drag, was smaller at α=2.5° than at α=0° because of a decreased relative upsweep angle of the rear part of the fuselage; consequently, the vorticity contribution was also reduced.

The drag coefficient of the fuselage itself, when taking into account the belly fairing and the truncated wings, was similar to the one recorded for the "Fuselage with horizontal stabilizer" configuration, according that the fuselage was set at 0°. Nevertheless, the vorticity was stronger, almost 3% of the total drag coefficient of the fuselage, which was much higher than what had been recorded without wings.

Boundary layer surveys

Boundary layer surveys have been performed at different streamwise locations on either the upper and lower symmetry lines or lateral lines, with the LDA system operating in the forward- or backward-scattering mode, respectively.

Profiles were plotted in a coordinate system associated with the boundary layer: y_n is the direction normal to the wall, X and Z are in the plane, tangent to the wall, with X in the direction of the free stream velocity.

Some mean and fluctuating velocity profiles are going to be discussed below; they correspond to the locations marked with the symbol • in figure 13.

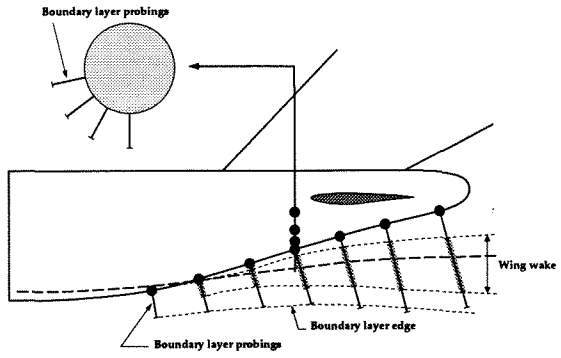

Figure 13: *Locations of some of the boundary layer surveys.*

Along the symmetry lines:

For these measurements, the LDA system was operated in the forward-scattering mode in order to obtain better accuracy, better measurement quickness and a better near wall approach.

On the lower symmetry line, seven measurement stations were defined between X/l=0.771 and 0.980. At each station, probings were performed in the direction normal to the wall. Mean velocity profiles are plotted in figures 14 and 15. The W-velocity component in the Z-direction, did not exceed 5 ms^{-1}, while the external free stream velocity is close to 260 ms^{-1}. Thus, that allows to verify, first of all the perfect symmetry of the flow and, secondly, that the measurement volume has been correctly positioned. The V-component was, in that case, not negligible; its intensity was straightly related to the thickening of the boundary layer due mainly to the downwash of the external flow.

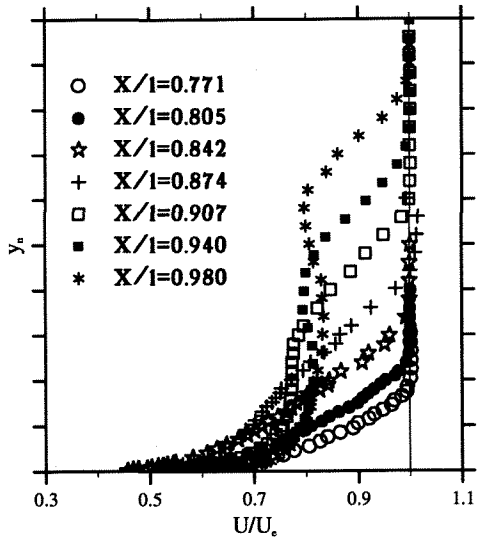

Figure 14: *Streamwise velocity profiles along the lower symmetry line.*

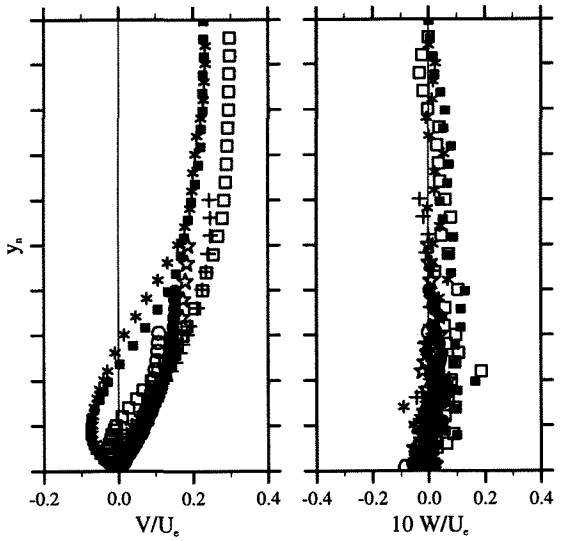

Figure 15: *Mean velocity components in the Y- and Z-directions along the lower symmetry line; same symbols as in figure 14.*

Downstream of X/l=0.842, the wake, coming from the trailing edge of the tip-truncated wings, began to interact with the mean streamwise velocity component, whilst the V-component did not seem to be too much

altered. As we moved downwards the rear end of the fuselage, that interaction went away from the wall, since the wing-wake separated from the lower symmetry line.

Therefore, the thickness of the boundary layer was rather important as compared to the greatest length of the fuselage cross-section. The consideration of boundary layer codes to predict the viscous flow in that region could thus be questioned. From these probings, it has been possible to estimate the wake from the wing/fuselage junction and its interference with the boundary layer developing along the lower symmetry line (cf. figure 13).

Along that symmetry line, the shear stress profiles ($-\overline{u'v'}$) were very altered (figure 16): this could be explained by the tridimensionality of the flow (convergence of external streamlines and divergence of wall streamlines) and the thickening of the viscous layer rather than the streamwise pressure gradient.

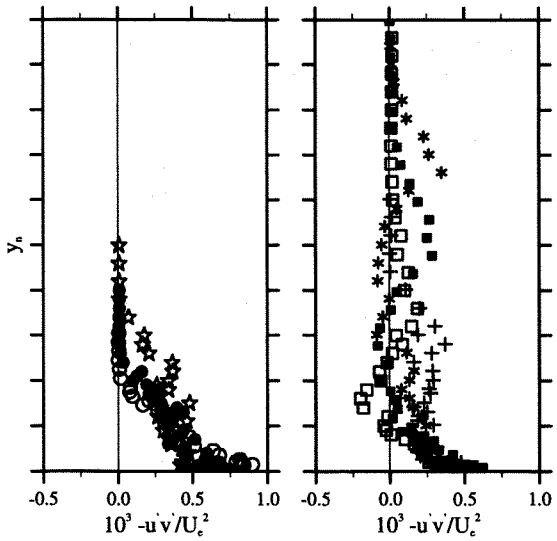

Figure 16: *Shear stress profiles along the lower symmetry line; same symbols as in figure 14.*

Downstream of X/l=0.842, the values of the shear stress were very small; therefore, the footprint of the wake coming from the wings/fuselage junction is clearly apparent on those profiles.

Along some lateral lines:

Furthermore, boundary layer surveys have been performed ahead of and just below the horizontal stabilizer, in different azimuthal lines; the location of these stations was judiciously selected, according to the wall streamline pattern, in areas of strong convergence of fluid.

The three components of the velocity, computed in the coordinate system associated with the external streamline, are plotted for various azimuthal angles at X/l=0.874 (figure 17), where θ=0° and 90° refer to the lower symmetry line and the mid-lateral line, respectively.

Comparisons have been performed between forward- and backward-scattering on the lower symmetry line; for that specific survey, it has been possible to go as close as 1 mm to the wall through backward-scattering. The agreement is rather good between these two laser configurations for θ=0°. Some discrepancies existed for the streamwise velocity component; moreover, the transverse component, W, was for sure weak but not equal to zero, as symmetry would require. This shows the existing difficulties to measure either small quantities or transverse velocities through backward scattering.

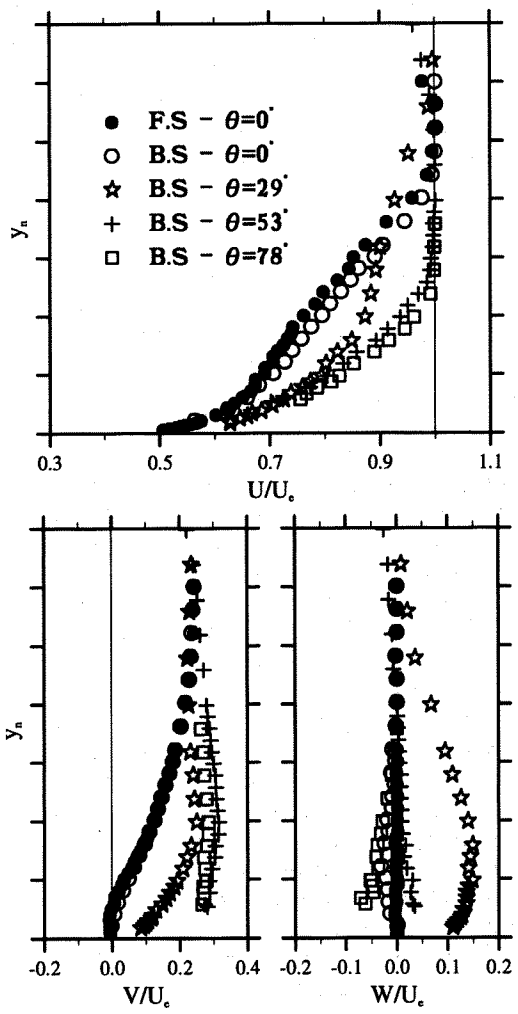

Figure 17: *X-, Y- and Z-components of the mean velocity at X/l=0.874 and different azimuthal locations.*

Nevertheless, such a method is of prime importance when dealing with change of sign of cross-flow, which was the case between azimuthal angles of 53° and 78°. These surveys allowed to show, first of all, the interaction with the wing-wake and, secondly, the rapid thickening of the turbulent boundary layer, when moving towards the lower symmetry line. For the high values of θ, in areas where visualisations revealed a strong convergence of wall flow, the V-component was rather strong; the growth of the boundary layer, which could have been derived, was not exagerated, yet.

Conclusions

Thus, these experiments were aimed at scrutinizing the viscous and inviscid flows in the rear part of

the fuselage and in the near wake, for a wing-body configuration. Detailed information has been devoted to point out the strong interaction between the wake coming from the tip-truncated wings and the boundary layer developing along the fuselage and also to characterize the effect of the horizontal stabilizer on the wall flow.

Tests were performed on a 1/80th scale model of a modern, transonic transport aircraft, in the transonic, pressurized wind tunnel with self-adaptive walls of CERT. The model consisted of a fuselage, a detachable horizontal rear stabilizer, a belly fairing and tip-truncated wings. Because of the size of the wind tunnel cross section, the real wing sized at the right scale, could not be considered; so, tip-truncated wings were computed by Aerospatiale in order to reproduce the correct downwash in the fuselage region.

The complete model was handled within the test-section by means of a fin-sting and was set at an angle of attack of 2.5°, while the horizontal stabilizer was fixed at -2° with respect to the Reference Horizontal Fuselage line. The tests conditions consisted of a stagnation pressure close to 2.1 bar, ambient temperature and a free-stream Mach number of 0.82.

Great care has been taken in order to ensure the correct pressure distribution on the model. The upper and lower flexible walls have been moved not only to take into account the presence of the model and of the walls boundary layers, but also to counteract the disturbance caused by the sting.

The combination of techniques such as oil-flow visualisation, boundary layer surveys, wake flow measurements has been a very powerful tool to get a very precise description of the wall flow and of the vortex motion that develops near the lower symmetry line of the fuselage and, consequently, spreads downstream of the upswept fuselage. A tremendous amount of data have been elaborated, that will help for validation or improvement of boundary layer as well as Navier-Stokes codes, as far as such complete wing-body configurations could be computed...

Areas of strong cross-flow associated with convergence of wall streamlines were well derived from oil-flow visualisations. Boundary layer surveys on specific lines pointed out the thickening of the boundary layer along the lower symmetry line of the model as well as an important wing-wake/fuselage-boundary layer interaction. Rear fuselage flow is generally dominated by three-dimensional separation i.e. convergence of wall streamlines, the rear fuselage upsweep creating a lift induced vortex system amplified by the wing downwash.

In the wake of the model, strong pressure losses were recorded; the use of a three-dimensional LDA system allowed to define more precisely both the vortex system associated with these velocity defect pockets and the intensity of the secondary velocity components in some confined areas of the whole wake.

When dealing with transport aircraft applications, besides friction or lift-induced drag reductions, benefits can be obtained via reduced fuselage afterbody drag;[10] following on results from the present investigation, interest might be to control the vortex flow by using small passive devices such as vortex generators or small fences. The goal sought after would be to act directly on the viscous flow developing between the lateral mid-line and the lower symmetry line of the fuselage and maybe indirectly on the flow along the horizontal tail.

Nevertheless, if one thinks to reduce the vorticity drag, whatever its contribution to the drag budget is, those hopefully successful passive devices could also modify consequently the pressure and friction drags and thereby produce a greater effect in terms of variations of the total drag of the fuselage.

On the other hand, benefits for aircraft applications could also be obtained from vortex flow control by reducing and/or confining instabilities that vortices could give birth to.

It is worth mentioning that the tests reported in this paper have been followed up by further experiments, where two different kinds of devices have been considered: small rectangular fences and small triangular vortex generators. The former act essentially on the external flow by driving it and trying to re-set upwards the external flow, while the latter act upon the wall flow, increase the turbulent mixing between the outer and inner regions of the boundary layer.

Those preliminary experiments show the possibility, first of all, to interfere with the convergence of wall streamlines and thus flow separation, secondly to modify locally the pressure distribution and, at last, to alter more or less significantly the shape of the wake as well as the distribution of the defect velocity pockets. Whatever configuration is concerned, it does not seem possible to suppress the global rear-fuselage vortex system, but to diminish it more or less; that system is due to the upswept fuselage and cannot be removed without changing the geometrical shape of the rear-part of the fuselage.

Acknowledgements:
The authors gratefully acknowledge the support that Airbus Industrie and the Service Technique des Programmes Aéronautiques have provided for the experimental research reported in this article.

References

[1] Coustols E., Prudhomme S., Destarac D., and Mignosi A. Rear fuselage flow studies on a modern transonic transport aircraft. In *Proceedings ICAS 19th Congress/AIAA Aircraft Systems Conference*, pages 1258–1271. Anaheim USA, September 1994. Paper 94-5.4.5.

[2] Coustols E., Prudhomme S., Mignosi A., and Destarac D. Rear fuselage flow studies on a modern transonic transport aircraft. *Journal of Aircraft*, 32(6):1183–1190, November-December 1995.

[3] Séraudie A., Archambaud J.-P., Blanchard A., Dor J.-B., and Mignosi A. T2 cryogenic transonic wind tunnel thermal design and control of the facility including models adapted for short run processing. In *Proccedings 3rd ASME-JSME Thermal Engineering Joint Conference on Cryogenic Wind Tunnels*, pages 379–386. Reno USA, March 1991.

[4] Archambaud J-P. and Mignosi A. The cryogenic adaptive wall wind tunnel T2: quality of the adaptation with 2D and 3D strategy, residual corrections, assessment of sidewall effect in 2D cases. In *International Conference on Adaptive Wall Wind Tunnel Research and Wall Interference Correction.* Xian China, June 1991.

[5] Archambaud J-P. and Mignosi A. Techniques d'adaptation tridimensionnelle à la soufflerie transsonique T2 de l'ONERA/CERT. Technical report, DERAT No 49/5606.34, April 1992.

[6] Prudhomme S., Séraudie A., and Mignosi A. A recent 3D laser doppler application at the T2 transonic wind tunnel: optimisation, experimental results and measurement accuracy. In *4th International Conference on Laser Anemometry.* Cleveland USA, August 1991.

[7] Mignosi A., Séraudie A., and Prudhomme S. Applications tridimensionnelles de la vélocimétrie laser en écoulement transsonique à la soufflerie T2. In *3ème Congrès Francophone de Vélocimétrie Laser.* Toulouse France, September 1992.

[8] Lépinard G. and Collin P. Design of a tip-truncated wing for a wind tunnel model. Technical Report 443.551/91, Aérospatiale, July 1991.

[9] Rivoire V. and Eichel P. Méthode d'analyse tridimensionnelle de systèmes hypersustentateurs. Technical report, Note Technique Aérospatiale 443.528/87, July 1987.

[10] Coustols E. Control of turbulent flows for skin friction drag reduction. to be published in Springer Verlag "Control of Flow Instabilities and Unsteady Flows" (ed. Meier G.E.A. & Schnerr G.H.), 1996. Advanced School - C.I.S.M Udine Italy - September 1995.